Microelectronic Engineering 95 (2012) 65–70

Contents lists available at SciVerse ScienceDirect

Microelectronic Engineering

journal homepage: www.elsevier.com/locate/mee

A pumping actuator implemented on a PCB substrate by employing water electrolysis

D.N. Pagonis [a,*], A. Petropoulos [b], G. Kaltsas [b]

[a] Department of Naval Architecture, TEI of Athens, 12210 Athens, Greece
[b] Department of Electronics, TEI of Athens, 12210 Athens, Greece

ARTICLE INFO

Article history:
Received 28 November 2011
Received in revised form 21 January 2012
Accepted 7 February 2012
Available online 16 February 2012

Keywords:
Electrolysis
Microfluidic systems
Actuator
Micro-pump

ABSTRACT

This work concerns the development of a novel actuator based on water electrolysis for pumping use in microfluidic systems. The electrolysis is performed inside a confined reservoir integrated on a PCB substrate which is connected to a microchannel. During the electrolysis process, the generated gases within the enclosed structure lead to a significant pressure increase which can be employed in order to move a liquid inside the microchannel. In order to demonstrate the device's principle of operation, water is driven through a meander microchannel structure which is connected at the output of an appropriate micro-tank; the effectiveness of employing electrolysis as an actuating principle has been investigated by monitoring the resulting pressure increase for a device with a larger reservoir. Furthermore, the operation of such a device as a micro-pump was successfully demonstrated by extracting the resulting flow-rate experimentally; the obtained results from the first prototype are clearly promising.

© 2012 Elsevier B.V. All rights reserved.

1. Introduction

Electrolysis is a well-known process for producing oxygen and hydrogen gases from water; its main advantages are the low power consumption and minimum heat dissipation. The idea of employing electrolysis as an actuation principle has already been exploited in various applications. Successful efforts have been reported in the past where substantial pneumatic energy was obtained by performing electrolysis of water in a confined space [1] and employing this energy for moving a diaphragm [2,3] or a probe [4]. Fabrication of a silicon micromachined micro-pump based on electrolysis [5–7] and employing it as a part of a micro-dosing system in the nanoliter range [8] has also been reported, while most recently challenging efforts towards the fabrication of implantable devices whose operation is based on electrolysis are appearing [9,10].

In the early 90's the concept of micro total analysis systems-μTAS was introduced [11,12] leading to the appearance of numerous pharmaceutical and biological applications; the main advantages of miniaturization of chemical assays include reduction of the required quantities of sample and reagents, faster response, automated operation and portability [13]. As μTAS systems evolved, their field of applications expanded. For example, successfully creating microsystems in order to perform polymerase chain reaction-PCR [14], a significant technique in genetic analysis, has been the subject of analysis in numerous research papers, which appear over a long time-span; devices of this type were firstly reported in 1993 and 1994 by Northrup et al. and Wilding et al., respectively [15,16]. Such systems, also called PCR-microfluidic chips, have evolved from simple microfluidic components to highly integrated systems [17].

A significant challenge to overcome in all the above mentioned systems, is concerning the controllable transport and pumping of quantities of biological fluids in the scale of microliters per minute. In order to tackle this hassle numerous efforts have been reported in the literature towards the fabrication of appropriate micro-pumps. The first reported micro-pump appeared over twenty years ago; it was fabricated employing silicon micromachining while its principle of operation was based on the piezoelectric or thermo-pneumatic actuation of a thin membrane [18]. The majority of micro-pumps can be categorized in two main groups [19]: mechanical with moving parts (employing reciprocating and peristaltic movement) and non-mechanical without the presence of moving parts (electrokinetic, magnetohydrodynamic, electrochemical, acoustic-wave, surface tension and capillary micro-pumps). In the case of mechanical pumps one can categorize them according to the actuation principle employed (piezoelectric, pneumatic, thermopneumatic, electrostatic, electromagnetic pump, etc.). We should note that as systems like μTAS and PCR-microfluidic chips continue to evolve rapidly, there is an urgent need for micro-pumps exhibiting certain advantages. That is, micro-pumps which can be fabricated with simple process steps, at low cost and thus disposable. These requirements can be met if plastic materials were

* Corresponding author.
E-mail address: d.n.pagonis@teiath.gr (D.N. Pagonis).

0167-9317/$ - see front matter © 2012 Elsevier B.V. All rights reserved.
doi:10.1016/j.mee.2012.02.006

employed for the fabrication of micro-pumps [20]. Such kind of micro-pumps can also be used for biomedical applications in drug delivery, a sector that attracts a significant interest during the last years.

A certain category of devices that implements plastic material is based on Printed Circuit Boards (PCB) and is often termed PCB-MEMS. In detail, Aracil et al. [21] have reported the successful fabrication of a low cost and single-use impulsion microdevice which can be easily integrated in complex microfluidic systems. The device is used for the injection or extraction of fluids and is fabricated based on a combination of SU8 and PCB-MEMS technologies. Our group has also presented in the past a polymer-based microfluidic flow sensor which is based on PCB-MEMS technology [22], whereby microchannels made of SU8 are structured on the surface of the PCB substrate.

In this context, we present the use of PCB to serve as the substrate material, on which a water electrolysis-based actuator for microfluidic is fabricated. The materials and the fabrication process which are implemented in the specific device are compatible with the aforementioned fabrication technology, providing the possibility of integrating a full scale automated microfluidic delivery system, including all its main components (actuating/sensing elements and necessary driving electronics) in the same circuit board. The main intention of the current work is to manifest the validity of the specific actuation principle for use in such systems.

2. Fabrication procedure and principle of operation

In order to demonstrate the successful use of water electrolysis as an actuating principle the device presented in Fig. 1a has been fabricated. The device is comprised of a micro-tank of predefined dimensions connected in series with an appropriate meander microchannel structure. Only the micro-tank is filled with water solution prior to device operation. The two Cu structures that form the micro-tank walls are also the electrodes, necessary for the electrolysis process (Fig. 1b). The electrodes are in direct contact with the confined operating fluid.

The device fabrication process is shown in Fig. 2a. As we can see it is a simple process, involving only two main steps. The initial stage of the fabrication process concerns the formation of the Cu electrodes and the microchannel walls on the PCB. A commercially available board with photosensitive resist on its upper surface is implemented, this way reducing the fabrication stages and the associated cost of the final device. The formation of both the micro-tank and the microchannel walls on the PCB surface is achieved by a sequence of exposition, development stage and finally the chemical etching of the Cu layer of the PCB. The thickness of the Cu layer defines the thickness of the resulting structures, which in the present case was equal to 25 μm. Typical dimensions regarding the resulting micro-tank were: 12 mm in length, 1 mm in width and 25 μm in height, while the microchannels were: 64 mm in length, 1 mm in width and 25 μm in height. The electrode dimensions were equal to 12 mm in length and 2.5 mm in width.

In the next stage, sealing of both the micro-tank and the microchannel walls is performed. This is achieved by the use of a special sealing tape based in polyolefin (commercially available by 3M).

In the resulting structure, it is merely the vertical sidewalls of the Cu electrodes that are exposed to electrolyte during the electrolysis process. We should mention that as a complementary step in the fabrication process, a thin Pt layer of approximately 3 nm can be deposited on top of the Cu tracks; although this step is not obligatory for the device's operation, it provides reasonable protection to the exposed areas of the Cu layer from corrosion during the electrolysis process.

The principle of operation of the proposed device is based on the electrolysis phenomenon. Electrolysis is a technique for converting electrical energy to pneumatic energy; in more detail, applying a certain voltage between two electrodes immersed in pure water leads to the production of hydrogen and oxygen gases at the negatively and positively biased electrode, respectively. The equations governing the gas production are as follows [1]:

Equilibrium equation representing the percentage of water that is always found as ionic species H^+ and OH^-:

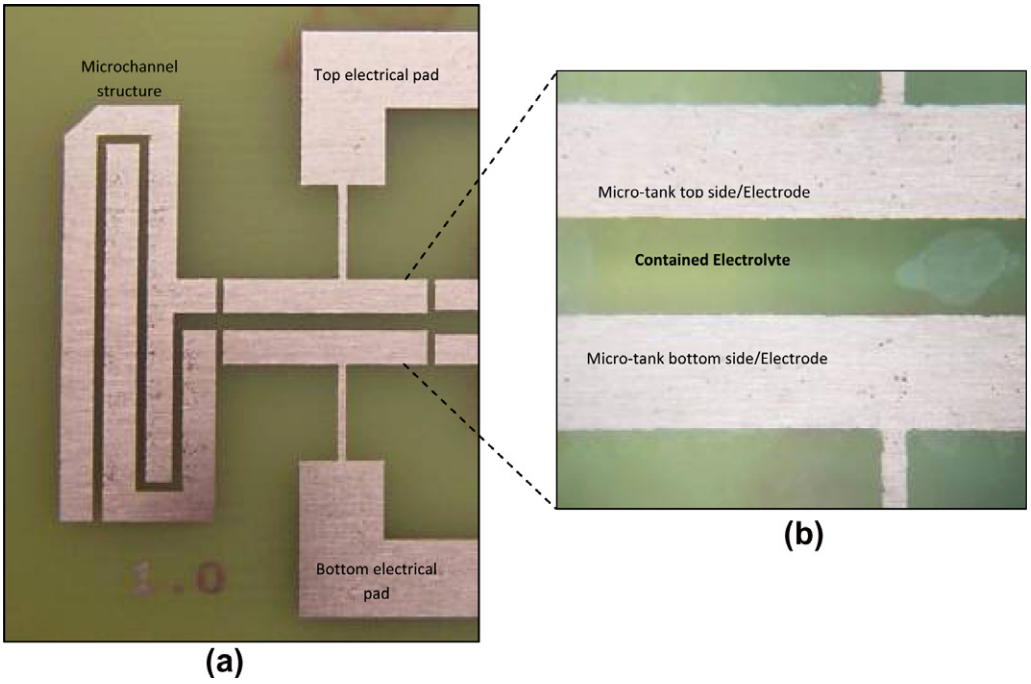

Fig. 1. (a) Top-view of the device; the micro-tank in series with the meander microchannel are illustrated (both are not sealed at this stage). (b) The sealed micro-tank filled with electrolyte. The two opposite sides comprise also the necessary electrodes for performing the electrolysis process.

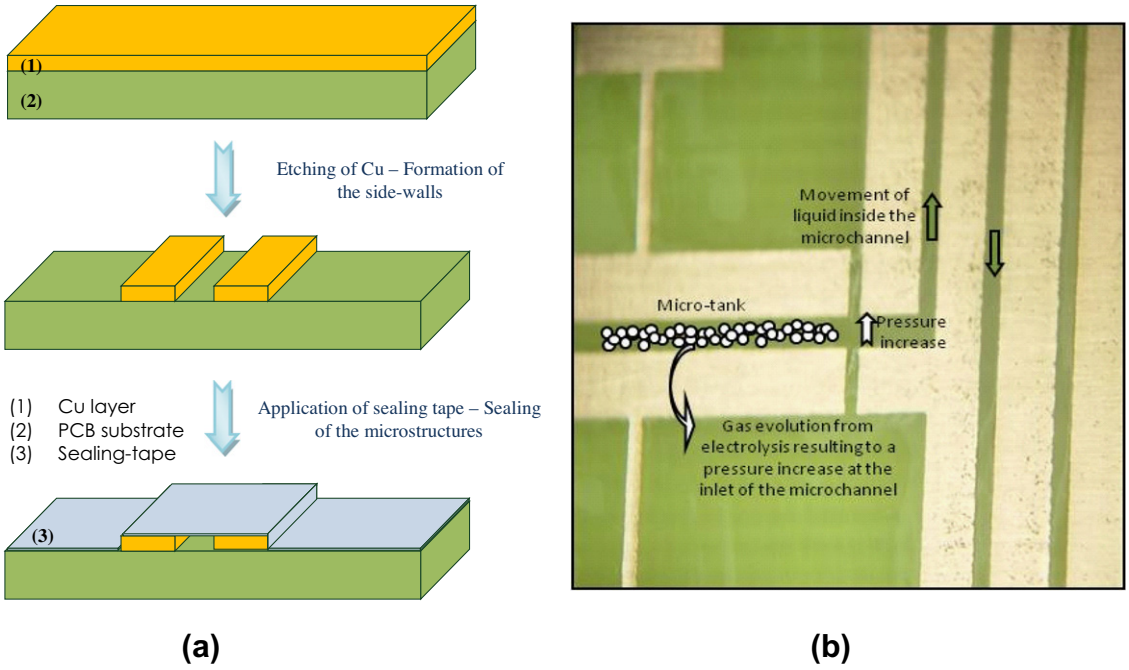

Fig. 2. (a) Outline of the fabrication process of the device. (b) Applying appropriate voltage/current between the two electrodes results to consequent movement of the liquid inside the micro-meander. The channel is sealed at the left-side in order to constrain the liquid flow in one-direction.

$$H_2O(l) \leftrightarrow H^+(aq) + OH^-(aq) \quad (1)$$

Generation of oxygen and hydrogen gases at noble metal electrodes:

$$4\ OH^- \leftrightarrow 2\ H_2O + O_2 + 4\ e^- \quad \text{at the anode} \quad (2)$$

$$2\ H^+(aq) + 2\ e^- \leftrightarrow H_2(g) \quad \text{at the cathode} \quad (3)$$

It is important to mention that the amount of gas evolved during electrolysis is directly related to the current passing through the electrodes while if it occurs in a confined space is capable of generating a pressure beyond 200 MPa [23].

In the case of the proposed device, applying a certain voltage to the integrated electrodes inside the micro-tank, results to the electrolysis of the contained electrolyte, as described above. Thus, by controlling the applied current passing through the electrodes and its duration, one can effectively control the rate and the duration of the production of gas at the electrodes, this way enabling the effective control of the pneumatic energy built-up inside the micro-tank. Since the inlet of the microchannel is connected in series with the micro-tank, the contained liquid is forced to move inside the micro-meander structure due to the build-up pressure. The above-described effect was confirmed experimentally by observing fluid movement inside the micro-meander after applying a low voltage (in the range of few volts) between the two electrodes, thus, proving the principle of operation of the device. In more detail, successful production of gas inside the micro-tank was observed, as well as subsequent movement of water entering the microchannel, due to the pressure increase induced (Fig. 2b).

We should note at this point that although the resulting sealing of the patterned Cu structure by employing the polyolefin based tape is quite conformal, the small gaps at the side of each of the electrodes-necessary for electrical isolation could potential lead to leakage of the liquid sideways. That is one of the reasons that after the successful demonstration of the use of water electrolysis as an actuating principle, a different design for the actuator was employed, as will be shown in the next section.

3. Experimental results and discussion

3.1. Electrolysis as an actuating principle – effectiveness evaluation

Having demonstrated the constructed device's operation principle, the effectiveness of employing electrolysis as an actuating mechanism was investigated, by direct monitoring of the pressure build-up inside the micro-tank. In order to allow for a more thorough study of the phenomenon, a Plexiglas micro-tank with dimensions 2.5 cm × 1 cm was glued on the surface of the PCB containing the Cu electrodes. The larger volume of the adopted tank in this case (1 ml capacity) allows for a higher pressure to be accumulated during electrolysis since the volume of the confined electrolyte inside the tank is maximized. An appropriate pair of tubes is adjusted on the upper tank wall serving as the inlet/outlet of the device, respectively. A view of the fabricated device is presented in Fig. 3.

We should note that in contrary to the structure described in the previous section, in the specific geometry the entire area of the patterned Cu structures residing inside the Plexiglas tank, act as electrodes during electrolysis, since this area is in direct contact with the corresponding liquid; for the specific device under test, each electrode has a surface of 12 mm^2.

The tank was filled initially with electrolyte though the inlet, which is then sealed, prior to the electrolysis stage. In order to measure the accumulating pressure inside the tank, a commercial pressure sensor (9510U by Spectre Sensors) was connected directly to the device's outlet. The sensor was connected to a PC via a serial interface enabling real-time monitoring and recording of the pressure values in the chamber.

During operation of the device, a constant electrolysis current I_e through time was applied at the electrodes. The recorded pressure increase is presented in Fig. 4 for three different I_e values (3 mA, 5 mA and 8 mA). As it can be noticed, the pressure inside the chamber is increasing almost at a constant rate, which is in agreement to the fact that the production of the gas inside the tank should be occurring at a constant rate since constant electrolysis current is

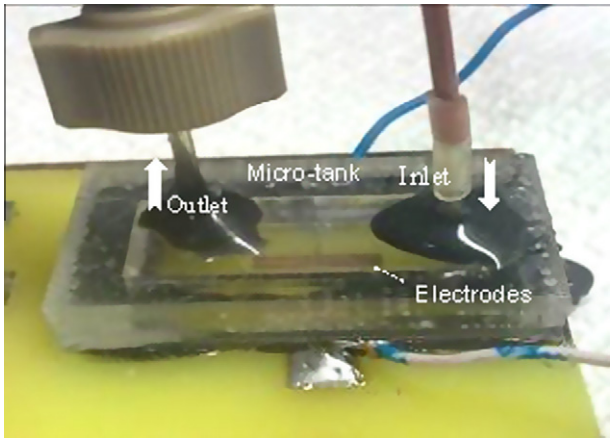

Fig. 3. View of the device employing a tank with a larger capacity.

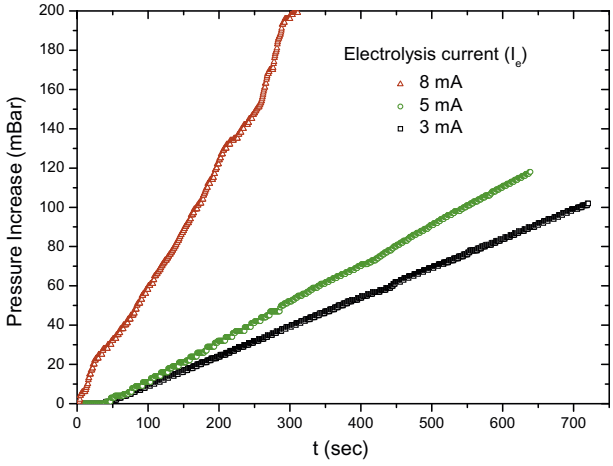

Fig. 4. Recorded pressure increase at the outlet of the device vs. time for different electrolysis current applied.

applied. It is also observed that, for the cases where relatively low electrolysis current is applied (3 mA and 5 mA), the pressure increase ΔP_e is developing linearly as a function of time, with corresponding rates of 0.148 mbar/s and 0.195 mbar/s, respectively. This linearity is expected since the electrolysis current is constant and no recombination of H_2O occurs inside the tank.

Thus a controlled pressure increase inside the chamber can be achieved by applying a predefined constant electrolysis current I_e, throughout a well specified amount of time. In the case of I_e = 8 mA, a deviation from linearity between ΔP_e and t is observed. This implies that for larger operating currents, increased errors may be introduced (i.e. leakage due to the large magnitude of pressure in the confined reservoir). However in the specific case, a significant pressure increase of 200 mBar was rapidly developed (in merely 5 min), which corresponds to a pressure increase rate of 0.628 mBar/s. We should mention that according to BoEhm et al. [8] assuming that all generated gas evolves in the form of gas bubbles, it can be proven that the total volume of gas generated during electrolysis depends linearly on the injected electrical charge Q (Cb). Thus one can expect that a linear relationship between the pressure increase rate and the applied current should be developed. If we compare the two pressure increase rates at Fig. 4, corresponding for electrolysis currents of 3 mA and 5 mA, respectively, we notice that this linearity is not observed; a possible reason could be improper impletion of the reservoir before operating the device, resulting to the presence of an initial volume of air inside the reservoir-different for each case; moreover the developed pressure increase is not direct proportional to electrolysis current since in order to start the electrolysis process is necessary to overcome a certain energy barrier [1]. Further experimental data though should be obtained in order to reach to a solid conclusion.

3.2. Pumping operation and determination of the resulting flow rate – discussion

Having measured the pneumatic build-up pressure for the constructed device successfully, the next step is the evaluation of its pumping ability. The experimental set-up used is presented in Fig. 5; in more detail, the outflow of the actuator is now connected to a 50 cm long micro-tube which is graduated in mm order. Initially, the tank of the device is filled with water through the inlet while the graduated part of the micro-tube remains empty. During operation of the device, the inlet valve is closed, and a constant current I_e is applied to the device's electrodes. The built-up pressure at its outflow results to water movement inside the marked section of the micro-tube. By measuring the time required for the water's front to cover the distance in between pre-determined marks, the fluid velocity is deduced.

The obtained results showing the pumped fluid propagation over time for various values of the operating current I_e are presented in Fig. 6. The fluid velocity can be deduced by the slope of the linear fit curve – as derived by the least squares method, for each group of experimental data. An almost linear increase of the resulting fluid velocity with respect to the current I_e (i.e. gas formation rate during electrolysis) is noticed, as expected. The value of the velocity measured ranges from 1.7×10^{-3} m/s to 11.1×10^{-3} m/s. Taking into account the micro-tube diameter which is equal to 500 μm, the above velocity range corresponds to a flow rate range from 20 μL/min to 135 μL/min. We should mention that the specific measured values correspond to the maximum developed flow rate $-Q_{max}$ when no pressure difference is present at the outflow of the device. Thus, the above results, give us only a preliminary evaluation of the prototype's operation. A more detailed analysis determining the pump's working point will be implemented in future research work.

Based on the specific data, the micro-pump-generated flow rate and the corresponding flow velocity as functions of the operating current are depicted in Fig. 7. The errors bars of the graph result from the standard deviation of the linear fit performed on the measurement data (Fig. 6). A linear relationship holds between the flow rate and the operating current, within the range of 3–12 mA. As the operating current value decreases, it reaches a certain limit (I_{limit} = 1.23 mA) below which no electrolysis is performed as mentioned above; thus no gas generation occurs which is illustrated as flat line behavior in the corresponding figure.

The resulting flow rate is presented in Fig. 7; the error magnitude is derived by the slope error calculated by the least squares method, previously employed in Fig. 6.

During the operation of the device, the value of the voltage difference across its terminals is almost constant and equal to 3 V. Thus, the corresponding power consumption for the given operation conditions is between 9 mW (given an operating current of 3 mA) and 36 mW (corresponding to an operating current of 12 mA).

The described procedure for measuring the water velocity is sensitive to experimental errors, since the exact determination of the water's front reaching each mark is based solely on observation. However, the employed method is a very simple and effective way for an initial estimation of the resulting flow rate. We should note that during continuous operation of the device, significant

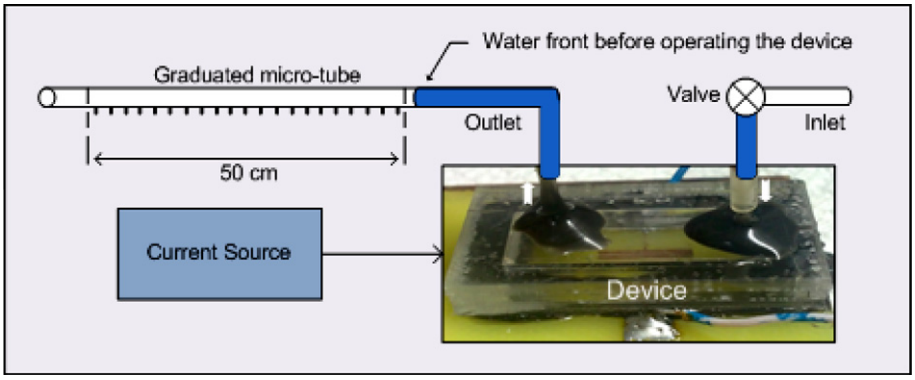

Fig. 5. Experimental set-up employed for determining the resulting flow rate at the outlet of the device.

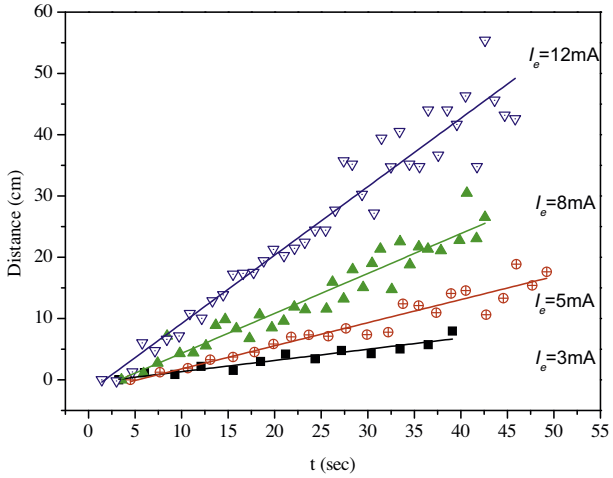

Fig. 6. The distance covered by the pumped fluid over time for different operating currents I_e of the device; the fluid velocity can be deduced by the slope of the linear fit curve for each group of experimental data. The large dispersion of the experimental data is mainly due to the poor precision of the measuring method.

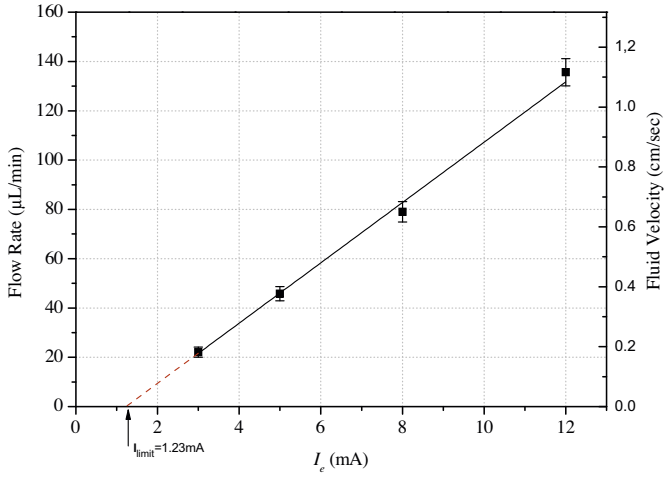

Fig. 7. The deduced fluid velocity and corresponding fluid flow rate as functions of the operating current I_e. A linear relationship holds between the specific quantities, which is due to the linear relationship between the generated volume of gas and the current applied during electrolysis. As the operating current value decreases, it reaches a certain limit (I_{limit} = 1.23 mA) below which no electrolysis is performed.

corrosion of the Cu electrodes was observed, due to the presence of oxygen inside the chamber, reducing, respectively the device's operating lifetime to the order of some hours. If the protective thin Pt layer is not deposed on top of the electrodes, the above mentioned lifetime is reduced to half its value. A feasible solution to overcome the specific problem would be to fabricate the electrodes by a different material such as Pt or Au.

Future research work concerns investigating the effect of the device's main parameters affecting its performance, such as the electrode geometry and the volume of the contained electrolyte. The geometry of the chamber is also a parameter that should be studied further, as well as the electrodes material which may significantly increase the device's lifetime as mentioned above. Furthermore, future work also involves the determination of the resulting flow rate in a more accurate way by connecting the actuator in series with the PCB microfluidic flow sensor developed by our group [22]. This will allow us to exploit in more depth the developed actuator's pumping characteristics such as the maximum pressure induced on no-flow conditions, leading to the determination of the device's optimum working conditions. The potential fabrication of valves/microfluidic sensors in the same substrate with the proposed device, is also included in future research work, thus forming a multi-functional integrated microfluidic system.

4. Conclusions

A PCB integrated actuator based on electrolysis was fabricated and successfully employed as a micro-pump. Its principle of operation was successfully demonstrated, while the effectiveness of employing electrolysis as an actuating mechanism was determined. A large pneumatic pressure increase occurring at a short time interval at the device's outflow has been recorded, suggesting a promising performance. Furthermore, the resulting flow rate was experimentally investigated with respect to the electrolysis current applied and a range from 20 μL/min to 135 μL/min was extracted. The proposed device employing PCB-MEMS technology combines important features such as simplicity, reduced fabrication time and cost as well as direct electrical communication to the macro-world.

References

[1] C. Neagu, H. Jansen, H. Gardeniers, M. Elwenspoek, Mechatronics 10 (2000) 571–581.
[2] C.R. Neagu, J.G.E. Gardeniers, M. Elwenspoek, J.J. Kelly, Journal of Microelectrocechanical Systems 5 (1) (1996) 2–9.
[3] C. Pang, Y-C. Tai, J.W. Burdick, R.A. Andersen, Nanotechnology 17 (2006) S64–S68.
[4] C. Pang, Y.C. Tail, J.W. Burdick, R.A. Andersen, Electrolysis-based parylene balloon actuators for movable neural probes, in: Proceedings of the 2nd IEEE International Conference on Nano/Micro Engineered and Molecular Systems, January 16–19, 2007, Bangkok, Thailand.
[5] S. BoEhm, W. Olthuis, P. Bergveld, J. Biomed. Microdev. 1 (2) (1999) 121–130.

[6] R. Sheybani, E. Meng, High efficiency wireless electrochemical actuators: design, fabrication and characterization by electrochemical impedance spectroscopy, MEMS 2011, Cancun, Mexico, January 23–27, 2011.
[7] Y. Chiang, M.J. Cima, T. Chin, Electrochemical actuator, European Patent Application 11151984.9, EP 2366896A2, September (2011).
[8] S. BoEhm, B. Timmer, W. Olthuis, P. Bergveld, J. Micromech. Microeng. 10 (2000) 498–504.
[9] Po-Ying Li et al., J. Microelectromech. Syst. 19 (1) (2010) 215–228.
[10] H. Gensler et al., Implantable MEMS drug delivery device for cancer radiation reduction, MEMS 2010, Hong Kong, January 24–28, 2010.
[11] A. Manz, N. Graber, H.M. Widmer, Sens. Actuators B Chem. 1 (1990) 244–248.
[12] A. Manz et al., Trends Anal. Chem. 10 (1991) 144–149.
[13] D.J. Laser, J.G. Santiago, J. Micromech. Microeng. 14 (2004) R35–R64.
[14] R.K. Saiki et al., Science 230 (1985) 1350–1354.
[15] M.A. Northrup, M.T. Ching, R.M. White, R.T. Watson, DNA amplification in a microfabricated reaction chamber, in: Proceedings of the Seventh International Conference on Solid-State Sensors and Actuators (Transducers '93) 7–10 June, Yokohama, Japan (1993) 924–926.
[16] P. Wilding, M.A. Shoffner, L.J. Kricka, Clin. Chem. 40 (1994) 1815–1818.
[17] N.C. Cady, S. Stelick, M.V. Kunnavakkam, C.A. Batt, Sens. Actuators B Chem. 107 (2005) 332–341.
[18] H.T.G. van Lintel, F.C.M. van de Pol, S. Bouwstra, Sens. Actuators 15 (1988) 153–167.
[19] C. Zhang, D. Xing, Y. Li, Biotechnol. Adv. 25 (2007) 483–514.
[20] C. Yamahata, M. Chastellain, V.K. Parashar, A. Petri, H. Hofmann, M.A.M. Gijs, J. Microelectromech. Syst. 14 (1) (2005) 96–102.
[21] C. Aracil, J.M. Quero, A. Luque, J.M. Moreno, F. Perdigones, Sens. Actuators A 163 (2010) 247–254.
[22] K. Kontakis, A. Petropoulos, G. Kaltsas, T. Speliotis, E. Gogolides, Microelect. Eng. 86 (2009) 1382–1384.
[23] C.G. Cameron, M.S. Freund, PNAS 99 (2002) 7827–7831.